HHS Public Access

Author manuscript

J Neuroimaging. Author manuscript; available in PMC 2023 September 01.

Published in final edited form as:

J Neuroimaging. 2022 September ; 32(5): 956–967. doi:10.1111/jon.13023.

Novel imaging markers for altered cerebrovascular morphology in aging, stroke, and Alzheimer's disease

Aditi Deshpande[1], **Jordan Elliott**[1], **Nitya Kari**[1], **Bin Jiang**[2], **Patrik Michel**[3], **Nima Toosizadeh**[1,4], **Pouya Tahsili Fahadan**[5,6], **Chelsea Kidwell**[7], **Max Wintermark**[2], **Kaveh Laksari**[1,8]

[1]Department of Biomedical Engineering, University of Arizona

[2]Department of Radiology, Stanford University

[3]Department of Neurology, Centre Hospitalier Universitaire Vaudois, Lausanne, Switzerland

[4]Arizona Center on Aging, Department of Medicine, University of Arizona

[5]Neuroscience Intensive Care Unit, Medical Critical Care Service and Department of Medical Education, University of Virginia School of Medicine, Inova Fairfax Medical Campus

[6]Departments of Neurology, Johns Hopkins University School of Medicine

[7]Department of Neurology, University of Arizona

[8]Department of Aerospace and Mechanical Engineering, University of Arizona

Abstract

Background and Purpose: Altered brain vasculature is a key phenomenon in several neurologic disorders. This paper presents a quantitative assessment of vascular morphology in healthy and diseased adults including changes during aging and the anatomical variations in the Circle of Willis (CoW).

Methods: We used our novel automatic method to segment and extract geometric features of the cerebral vasculature from MR angiography scans of 175 healthy subjects, which were used to create a probabilistic atlas of cerebrovasculature and to study normal aging and inter-subject variations in CoW anatomy. Subsequently, we quantified and analyzed vascular alterations in 45 acute ischemic stroke (AIS) and 50 Alzheimer's disease (AD) patients, two prominent cerebrovascular and neurodegenerative disorders.

Results: In the sampled cohort, we determined that the CoW is fully formed in only 35% of healthy adults and found significantly ($p<0.05$) increased tortuosity and fractality, with increasing age and also with disease in both AIS and AD. We also found significantly lower vessel length, volume and number of branches in AIS patients, as expected. The AD cerebral vessels exhibited significantly smaller diameter and more complex branching patterns, compared to age-matched healthy adults. These changes were significantly heightened ($p<0.05$) between healthy, early onset mild AD and moderate/severe dementia groups.

Corresponding Author: Kaveh Laksari, klaksari@arizona.edu Phone: 520-621-4307, Address: 1230 N Cherry Ave. Tucson, AZ.

Conclusion: Although our study does not include longitudinal data due to paucity of such datasets, the specific geometric features and quantitative comparisons demonstrate the potential for using vascular morphology as a non-invasive imaging biomarker for neurologic disorders.

Keywords

cerebral vasculature; Stroke; Alzheimer's disease; imaging; aging; biomarkers

Introduction

Alterations in cerebral vasculature are common in the pathophysiology of many neurologic disorders. Acute ischemic stroke (AIS) and Alzheimer's disease (AD), the two most common cerebrovascular and neurodegenerative diseases, respectively, often coexist and are among the leading causes of mortality and morbidity worldwide.[1] Both conditions are hypothesized to possess significantly altered architecture of the brain vascular network.[2–4] These changes can often precede clinical symptoms and may serve as early disease markers.[5,6] Consequently, studying the quantitative and qualitative changes in the cerebral vascular network due to aging and disease is pertinent to understanding brain health and may impact diagnosis, and treatment of neurologic disorders.[7,8]

The reduced blood flow after AIS is coupled with a series of changes associated with structural remodeling of the cerebral vasculature that results in the vessel geometry quantitatively varying from the healthy vasculature.[9,10] Some of these changes may precede the clinical onset of the ischemic event in patients with atherosclerotic vessels.[11] Therefore, analysis of the brain vessel geometry can improve prognostication, facilitate studying therapeutic options and guide reperfusion therapies for AIS patients when feasible.[12] However, quantitative studies of structural changes in the cerebral vasculature before and immediately after stroke and their effects on clinical outcomes are lacking despite their importance as stated in epidemiological studies.

Despite our expanding knowledge of the significance of cerebrovascular alterations in AD at the cellular and microvascular level,[2] which is due to plaque and amyloid deposition as well as pathological structural alterations in the endothelium, our understanding of morphological changes in the major vessels in AD is still in early phases and has mainly been limited to animal studies.[5,13] Reduced cerebral blood flow (CBF) and perfusion, observed in neurodegenerative diseases, exacerbates neuronal degeneration and amyloid deposition, reduces elastin production, causes distensibility and autoregulation loss, and increases wall shear stress.[2,14] These developments could lead to significant morphological changes throughout the brain vasculature, including increased vascular stiffness, decreased diameters, and possibly higher tortuosity and fractality in AD brain vessels.[2,15,16] Therefore, stroke, atherosclerotic lesions, hypertension, and other cerebrovascular diseases are common comorbid factors for neurodegenerative disorders, in particular AD.[17] Consequently, research and diagnosis of these diseases can benefit greatly from a quantitative and qualitative analysis of the changes in the cerebral vascular network and structure in the corresponding populations.[8,18]

Analysis of the pathological alterations in the cerebral vascular network requires a deep understanding of healthy vascular morphology and the normal distribution of cerebral vessels. A vascular atlas with geometric features can be used to study and quantify the variations in vascular geometry within the healthy population. As shown by our previous study, vascular morphology can be characterized using geometric properties of the vessel network, such as tortuosity, fractality (quantified using fractal dimensions), branching pattern, average diameter, total length, and volume.[19] These properties have been shown to be corroborated indicators of vascular health and potential pathology.[8,19–21] Most brain atlases typically do not include detailed morphology of the brain vascular network due to inadequate vascular imaging data from a large sample of healthy subjects[22] and a lack of validated algorithms to segment, extract, and analyze cerebral vasculature. Instead, current cerebrovascular atlases are confined to only the CoW region and often exclude the more distal network, and also lack quantification of inter-subject variations.[22,23] Developing a comprehensive atlas of the cerebral vasculature containing quantitative geometric features, including distal branches of the intracranial vessel network and normal variations at different ages in the healthy population, is essential in understanding the brain's anatomy and physiology. It also enables assessment of compensatory collateral flow in the CoW and the collateral circulation during acute and chronic ischemic conditions, given their vital role in the distribution of CBF, to assist with early diagnosis, optimal reperfusion approach, and patient outcomes prediction.[11,12]

Here we present a probabilistic atlas of the healthy human cerebral vasculature, labeled based on major cerebrovascular territories, to define the pattern of vessel distribution and quantify vascular geometric features. We utilized this atlas to study alterations in cerebrovascular geometry and inter-subject variations as well as vessel network modifications during natural aging. Additionally, we used the extracted 3D vessel networks and their morphometric features as measures to quantify "symmetry" between the left and right hemispheres within the brains of healthy adults as this hemispheric symmetry (or the lack of it) has been associated with various alterations in blood flow dynamics and can have significant implications in pathological conditions or even indicate a predilection of ischemic events in one hemisphere over the other.[24,25] We then applied the knowledge of healthy vascular morphology to study morphological alterations in AIS and AD, compared quantitatively to the age-matched healthy adult population to find potential hallmarks of these neurological disorders.

Methods

Retrospective datasets

This retrospective study uses previously collected and anonymized data from IRB approved studies, made publicly available or obtained upon acquiring consent.

We used magnetic resonance angiography (MRA) scans from 175 healthy subjects, 45 AIS, and 50 AD patients for this study (Table 1). Out of the 175 healthy subjects scans, 109 were obtained from the MIDAS public database, made available by the CASILab at the University of North Carolina at Chapel Hill and distributed by Kitware, Inc.[26] An Allegra 3T MR scanner (Siemens Medical Systems Inc., Germany) was used for data acquisition

with 3.56ms echo time, 35ms repetition time and 22 degree flip angle. The healthy atlas excludes subjects with a past medical history of hypertension, diabetes, or head trauma. The MRA scans of the remaining 66 healthy subjects and 50 AD patients were obtained from the OASIS-3 study, conducted by the Knight Alzheimer Research Imaging Program at Washington University.[27] The scans included in the OASIS-3 database were acquired on 3 different Siemens scanner models - a 1.5T scanner with a 16-channel head coil and two 3T scanners with a 20-channel head coil. The AD scans correspond to patients with varying dementia levels based on the Clinical Dementia Rating (CDR), including early-mild (CDR 0.5 or 1) and moderate-severe (CDR 2 or 3) dementia. To be graded on the CDR, participants completed clinical assessment protocols in accordance with National Alzheimer Coordinating Center Uniform Data Set and included family history of AD, medical history, physical examination, and neurological evaluation.[28] Finally, the MRA scans of the 46 AIS patients were obtained from the Centre Hospitalier Universitaire Vaudois in Lausanne, Switzerland, acquired on a 1.5T Siemen's scanner.

Segmentation and Registration

We used our recently developed and validated methodology to characterize vascular morphology from the imaging data.[19] Using automatic cerebral vascular segmentation, we extracted vessels as fine as the imaging resolution to determine the geometric properties of the segmented vascular network. Our segmentation method was previously validated using a realistic 3D model of the CoW anatomy with varying levels of added noise as well as imaging artifacts.[19] This method tracks connected tubular structures in 3D volumes and thus performs better under technical issues such as motion artifacts and inflow effects which can cause intensity inhomogeneities in imaging data than other freely available segmentation algorithms. The segmentation involves a multi-step process, resulting in a 3D binary volume of the vessel network, which is then skeletonized to obtain the centerlines of the vessels and the diameter at every point on the centerline. We then define a 'branching node' of the vascular tree as a point connected to 3 other points (i.e., a bifurcation). Using this definition, we calculated the global geometric features of the vessel tree as follows:

1. Total length: Total length of the vessel network calculated by summing the length of all the skeletal segments between 2 nodes.
2. Total number of branches: A 'branch' was defined as a sequence of points along the vessel beginning at a bifurcation point and ending either at the next bifurcation or at the last point on the vessel (in this case, it is a terminating branch).
3. Average and maximum branch length: The mean of the lengths (geodesic distance/length) of all branches in the network as well as the length of the longest branch found.
4. Average diameter: The mean of the diameter values at all points on the centerline
5. Total volume: Volume of the vessel network is calculated by considering the vessels as cylinders with a varying diameter along the total length.

6. Fractal dimension: The fractality of the vessels was determined using the box counting method. This feature can be used as a measure of morphological complexity in the cerebral vasculature.

7. Vessel tortuosity: Vessel tortuosity was defined using the sum of angles measurement (SOAM) between sets of 3 points on the centerline divided by the total length.

To provide a common standard space for comparison of all the scans in the study and account for the varying reference coordinates between different scanners and patient positions, each time-of-flight (ToF) MRA sequence and the corresponding segmentation were spatially normalized to the Montreal Neurological Institute (MNI) standard anatomical brain atlas reference space[29] with 0.5 mm^3 isotropic image resolution in three steps: first, each patient's ToF MRA sequences were registered to the corresponding T1-weighted imaging (T1) dataset via a rigid transformation. The T1 datasets were then registered to the T1 MNI brain atlas through an affine transformation. Finally, the two transformations were concatenated and multiplied to transform the segmented network directly into the reference space of the MNI brain atlas. The MNI atlas, adopted by the International Consortium of Brain Mapping, uses a series of 152 normal control MRI scans to define standard anatomy and consists of 'templates' for MRI sequences routinely used in both clinical and research settings to register MR data to common space.

Scans from the OASIS-3 database spanned a larger region of interest (ROI) from the top of the subject's head to approximately the middle of the neck region, whereas scans from the MIDAS database only consisted of the head region. To ensure our analysis spanned a uniform ROI within the brain, we selected a fixed volume from the OASIS-3 dataset by automatically selecting the first 140 slices starting from the top of the head.

Healthy cerebrovascular atlas and geometric feature analysis

We averaged the registered segmentations from the 175 healthy ToF scans to create the atlas of regional artery probability, with every pixel containing the probability of belonging to a vessel. We then extracted the average geometric features of the healthy brain vessel networks including vessel tortuosity, fractal dimension, number of branches, average and total branch length, and diameter.[19] The anatomical regions in the atlas were labeled based on major vascular territories, namely the left and right middle cerebral artery (MCA), the anterior cerebral artery (ACA) and the posterior cerebral artery (PCA). This labeled cerebrovascular atlas of the healthy population, including the averaged geometric features of the vessel network, was then used to study the variations in CoW in healthy subjects and vessel geometry due to aging, including a fully formed CoW and an absent or hypoplastic left and right anterior and posterior communicating arteries (ACoA and PCoA, respectively) and the first segment of the PCA (P1). Given its key role in maintaining CBF distribution and providing collateral blood flow, CoW variations can affect the clinical outcomes after a cerebrovascular event. To quantify aging-related changes in the vasculature, the healthy cohort was divided into six age groups: group 1 (< 29 years old, n=22), group 2 (30–39 years old, n=20), group 3 (40–49 years old, n=21), group 4 (50–59 years old, n=19), and group 5 (60–70 years old, n=29), and group 6 (>70 years old, n=19). To assess the required

sample size for a high-powered analysis, power analysis was performed for a desired power of 90. This was calculated based on the estimated effect size (>1 for all of the features which were significantly different) and the chosen p-value of 0.05[30].

We further studied intra-subject inter-hemispheric symmetry in vascular structure and quantified it as a percent difference using the extracted morphological features by dividing the registered segmentations into left and right sides along the sagittal midline. Additionally, the 3D Dice Similarity Coefficient was calculated as a symmetry metric to evaluate the similarity/overlap between each slice of the left vs. right hemispheric vessel volume.

To be included in the atlas, the scans of healthy subjects from the OASIS-3 database were resampled to 0.5 mm isotropic image resolution to match the scans from the MIDAS database. This avoids any discrepancy in the range of detected vessels in the averaged probabilistic atlas that could arise due to varying resolutions.

Quantifying alterations in vascular geometry in AIS patients

Emergent large vessel occlusion (LVO) strokes occur upon the occlusion of a major intracranial artery (ICA, M1, M2 segments of the MCA and Basilar) and significantly decrease CBF to large areas of the brain. Patients with LVO stroke are expected to show major deviations from the healthy atlas with a significant decrease in the number of branches, total length, and volume of the cerebral vasculature. Nevertheless, other geometric variations such as vessel tortuosity and fractality have not been studied yet. The stroke data consisted of 45 AIS patients with confirmed clinical and radiographic diagnosis of occlusion of the first (M1) and second (M2) segments of the MCA (n=24 and n=9, respectively) and the internal carotid artery (ICA, n=12), corresponding to the most common stroke syndromes in the average population.[31] We additionally defined a “vaso-deviation score” by determining how different each voxel of a patient’s specific vasculature is from its healthy counterpart in the atlas and normalizing this difference by the variance within the atlas. This has the potential of being used to automatically detect the presence and location of a large vessel occlusion in stroke patients since regions with a higher vaso-deviation score would correspond to the LVO location.[3,32]

Quantifying alterations in vascular geometry in AD patients

We hypothesized that the vasculature of AD patients possesses abnormally high branching and complexity with a higher tortuosity, fractal dimensions and number of branches, and a decreased average vessel diameter. We applied our validated segmentation and feature extraction method to MRA scans of 50 AD patients with varying levels of dementia, defined using the CDR scale[27] and extracted the cerebral vascular networks and their corresponding geometric properties. The quantitative extracted geometric features were compared to the healthy average morphometric features The data was then further divided into two – early-mild (CDR 0.5 and 1) and moderate-severe (CDR 2 and 3) dementia levels.[27] We tested for significant quantitative differences in the vasculature between AD patients versus healthy subjects as well as between patients with early-mild versus moderate-severe dementia.

Statistical analysis

When applicable, we conducted one-way ANOVA, followed by Tukey's post hoc test to assess changes in the vascular architecture across the age groups within healthy subjects. The comparison of stroke and healthy vasculature was performed for 45stroke patients, which were quantitatively compared against the healthy subjects from the atlas using the ANOVA test, after adjusting for age as a factor. Furthermore, the vascular networks of age-matched healthy controls and AD subjects were compared using the multi-way ANOVA between groups (healthy, early-mild AD, moderate-severe AD). The p-values were corrected by the Benjamini-Hochberg method to control for the false detection rate.[33]

Although we down-sampled the data of the 66 healthy subjects from the OASIS-3 dataset (from $0.3\times0.3\times0.3$ mm^3 to $0.5\times0.5\times0.5$ mm^3) to be included in the averaged probabilistic atlas and the normal aging study to increase the number of subjects, for comparison between healthy and diseased brains, we used the original resolution of each database since the finer resolution of the OASIS-3 dataset provides more granular information regarding the vascular network and the corresponding pathological changes due to AD. The morphometric features obtained from the stroke scans (imaged at $0.5 \times 0.5 \times 0.5$ mm^3) were only compared to those of healthy subjects from the MIDAS data (also imaged at $0.5 \times 0.5 \times 0.5$ mm^3), and the features of AD subjects (from the OASIS-3 database, imaged at $0.3 \times 0.3 \times 0.3$ mm^3) were compared only to the healthy subjects within the OASIS-3 dataset (also imaged at $0.3 \times 0.3 \times 0.3$ mm^3). Thus, no comparisons were made between imaging data of different resolutions.

Results

Healthy cerebrovascular atlas

The generated probabilistic cerebrovascular atlas displayed the major cerebral arteries based on occurrence in specific anatomical locations. The results were visually and quantitatively in accordance with the expected occurrence probabilities of regular cerebrovascular anatomy. The largest probabilities of occurrence were seen at the base of the ICA (immediately after bifurcation from common carotid artery), followed by the ICA bifurcations into bilateral MCAs and ACAs, and then the basilar artery (BA). Compared to the anterior circulation, the higher variation in the BA diameter in healthy adults resulted in scattered probability values. Figure 1 shows three axial slices of arterial probabilities overlaid on the corresponding axial T1 slices. The slices have been chosen from different axial locations as shown in the corresponding panel (purple inserts) ranging from the base of the CoW to superior regions of the brain. The color bar contains the raw values from the atlas map and represents voxels with varying probability of being on a vessel. With an expected reduction in vessel diameters and increased variation among individuals, the arterial occurrence probability decreased upon moving distally from the CoW.

Through power analysis, the minimum required sample size 'N' was determined to be 120 (with number of subjects per group, n, being ~20), leading to The Dice Similarity Coefficient metric to quantify the overlap/similarity between the vessel networks was found to be 0.23 ± 0.10 which demonstrates varying inter-subject similarity and low intra-subject overlap between the hemispheres.

Table 2 summarizes the geometric features extracted from 175 healthy subjects included in the statistical atlas (all at 0.5mm isotropic resolution). In the assessment of vascular symmetry between hemispheres, we found that the vascular geometry diverges between the 2 hemispheres at varying degrees with length, volume and branching having a higher percent difference than average diameter, fractal dimension and tortuosity (Table 2).

We found that the majority of the healthy subjects had a hypoplastic CoW – only 35% of the subjects had a fully formed CoW. Of our subject population, 40.5% missed at least one PCoA, 21% missed the ACoA, and 11% and 8% missed the A1 and P1 segments of the ACA and PCA, respectively. A smaller number of healthy adults missed one ACA (1%), P1 segment of the PCA (2%) or the PCoA (5%). We include the six most common presentations of the CoW anatomy within our dataset in Figure 2. The variations are found to be generated due to under-developed or missing segments in most cases.

Figure 3 includes the major findings of the changes in healthy vascular morphology with respect to increasing age. There was a significant increase across most age groups in the tortuosity ($p<0.001$), total length ($p<0.001$), number of branches ($p<0.001$), and fractal dimension ($p<0.001$) in a multi-group ANOVA. Post hoc analysis showed a significant increase in tortuosity and fractality with age which is consistent with our expectations. There was a significant increase in total vessel length with age which would be expected since there was also an increase in the number of branches. No significant overall change was observed in average diameter, average branch length or maximum branch length across the 6 age groups, spanning ages 19 to 84 years.

Vascular geometry in stroke patients

The geometric features of the cerebral vascular tree of 45 stroke patients compared to the healthy atlas of subjects and the average values for each geometric feature are presented in Table 3. As supported by our previously published preliminary findings,[19] cerebral vasculature is significantly altered in stroke patients compared to the healthy average, beyond the expected shorter total length (2.10±0.71 m vs. 3.19±0.67 m) and smaller volume (63.45±21.83 ml vs. 96.12±17.51 ml). Stroke brains were also found to possess higher tortuosity (5.80±0.92 vs. 3.24±0.57) and fractal dimension (1.79±0.2 vs. 1.55±0.29), alluding to atypical vessel remodeling, along with the expected findings of reduced number of branches, length, and volume.

Vascular geometry in AD patients

As hypothesized, the AD patients' vascular network is characterized by higher tortuosity and fractality, greater number of branches and a smaller average diameter. The association of these vascular structural alterations with disease were seen across the AD groups, when adjusted for age. As dementia levels increase from early-mild to moderate-severe, we observed significant differences in the vascular features between groups with varying levels of dementia, specifically higher tortuosity, fractality, number of branches, and a smaller average diameter. The quantitative information of the vascular geometric features for 50 patients with AD are reported in Table 4, including a comparison with healthy subjects. For visual assessment, Figure 4 shows the cerebral vascular network from 2 healthy subjects

and 2 AD patients and depicts the heightened tortuosity including looping and twisting in the vascular network of an AD patient. Such twists and loops are not observed in healthy subjects and is corroborated with studies which reported similar behavior of cerebral vessels in mice (6). Figure 5 shows plots of the significantly different features between the healthy and AD groups, namely the total length, fractal dimension, tortuosity, and average diameter.

Discussion

Both natural aging and disease alter the cerebrovascular network. These changes, from the cellular level to vessel wall deterioration and ultimately modified vascular architecture, contribute to the development and progression of neurologic disorders.[13,14] Therefore, a thorough understanding of cerebrovascular alterations such as increase in arterial stiffness, tortuosity, endothelial dysfunction and hypoperfusion, offers insight into the underlying pathophysiological pathways, natural course, and risk assessment of common and burdensome cerebrovascular and neurodegenerative diseases. A quantitative analysis of the cerebrovascular network may improve the timing and accuracy of diagnosis and provide an opportunity for preventive and early therapeutic interventions for individuals at risk for ischemic and hemorrhagic strokes, atherosclerosis, and dementia. The analysis of modified vascular structure with the natural aging process offers insight into the various pathways leading to these cerebrovascular alterations and possibly causing or exacerbating disease in older adults.[18] The comprehensive atlas of healthy cerebral vasculature enables quantitative characterization of the average “normal” population based on vascular geometry features. The healthy template for vessel distribution and geometrical patterns can enable clinicians and researchers to compare and analyze changes in the cerebrovascular network during aging and various pathological states. Additionally, studying the inter-hemispheric symmetry can help further our understanding of healthy vascular morphology and provide insight into varying cerebral hemodynamic response to ischemic events and also pathogenesis of cerebrovascular diseases and predisposition to such pathological occurrences in one hemisphere over the other.[24,34]

We found a significant age-related increase in vessel tortuosity and fractality that could be hypothesized to be attributed to the increased endothelial resistance, and in turn, an increased incidence of hypertension in older adults. An unexpected finding was the lack of significant group differences in average diameter, contrary to a previous report of increased vessel diameter by aging.[35] Although our study does not include longitudinal data, the analysis of modified vascular structure with the natural aging process offers insight into the various pathways leading to these cerebrovascular alterations and possibly causing or exacerbating disease in older adults. Additional studies including a larger sample size across all age groups or longitudinal data are warranted to elucidate this finding with implications in risk-stratification for cerebrovascular disorders.

The CoW plays a pivotal role in CBF distribution in both healthy and pathological conditions. For instance, the CoW anatomy, by governing collateral blood flow during AIS, can alter the natural course of ischemic core growth, salvageable penumbra, response to acute reperfusion therapies, and ultimately clinical outcomes.[36,37] However, the CoW anatomy varies considerably among individuals.[12,38] Therefore, we found it imperative to

quantify various anatomic presentations of the CoW in healthy adults. Using a database of 175 healthy subjects, we found that only 35% of individuals have a completely formed CoW, consistent with earlier reports, while the rest of the population present some anatomical variation in CoW anatomy.[12,38] This finding is primarily due to hypoplastic (underdeveloped) or aplastic (absent) rather than fused or additional vessel segments. This is of significance as CoW morphometry can provide insight into the patient's collateral circulation and risk of stroke, since missing segments of the CoW are associated with higher risk of stroke and an incomplete CoW has also been used as a predictor of Stroke.[39,40]

Though it is hypothesized that pathological vascular morphology is tied to AIS and there is structural remodeling of the vasculature before and after an ischemic event, little has been reported quantitatively. Most studies in literature have focused on cellular and molecular mechanisms of cerebrovascular remodeling, looking at endothelial dysfunction which can lead to vascular changes.[41,39] However, quantification of such effects is still lacking. Using the labeled healthy cerebrovascular atlas and the extracted cerebrovascular morphometry using the geometric features, we quantified the deviation in the vascular networks of stroke patients from the healthy population. Similar to our previous preliminary report,[19] we found significant differences in cerebrovascular geometry of stroke patients consisting of an expected decrease in total vessel length, volume, and number of branches along with an increased vessel tortuosity and fractality. These findings can be attributed to atypical vessel morphology in stroke patients. The deviations from healthy cerebrovascular geometry can serve as a diagnostic tool for automated stroke detection to complement the existing clinical and imaging capabilities, since significantly decreased vascular density, in the form of lower length, volume and branching, can indicate a large vessel occlusion.[42] Such a tool has several implications in both bedside and bench assessment and treatment of stroke patients. Analysis of vascular geometric features and comparing patient specific vascular maps to the atlas can enhance timing, sensitivity, and specificity of occlusion detection not only for proximal large vessels but also for distal medium vessels that may also be amenable to acute reperfusion treatments. These advantages are particularly important when there is a clinical equipoise or lack of access to subspecialized neuroradiologists to interpret multimodal advanced neuroimaging studies. Moreover, assessment of vascular morphology can improve the prediction of stroke patients' response to reperfusion therapies[9] and long-term clinical outcomes[43] since recent technological advances have expanded the application of endovascular thrombectomy as an increasingly effective treatment for AIS.[44] Interestingly, the altered vessel morphology may precede the ischemic event in stroke patients,[10,21,34,45] alluding to its possible application as an early marker for stroke occurrence and prevention, but this needs to be studied extensively in longitudinal studies with a larger dataset.

Neurodegenerative diseases, including AD, are characterized by irreversible and progressive neuronal loss. AD is increasingly recognized as a multifactorial disease with well-established vascular risk factors[46] and a key role for vascular dysfunction.[4,7,47,48] Neuritic plaques and vascular amyloid depositions, the early hallmarks of AD are associated with altered cerebral vasculature. Documented hypoperfusion in AD can initiate a vicious cycle of amyloid deposition, neurodegeneration, and cognitive decline.[2,14,49] Accordingly, vascular morphological changes have been reported in AD patients, with some changes

preceding clinical presentations. However, these changes have only been studied sparsely in animal models[5] or post mortem human subjects[15] and the literature is mostly limited to alterations in the microvasculature.[2] Using non-invasive MRA data, our quantitative analysis of vascular geometric differences in AD patients vs. healthy is the first study of its kind that quantifies abnormal macro-vasculature morphology in AD patients *in vivo*, using routine imaging data. We found higher vessel tortuosity and fractality in AD patients, compared to age-adjusted healthy subjects, associated with increasing levels of dementia. These findings agree with the previously hypothesized correlation between vessel stiffness and resistance, seen in AD patients, and structural vessel changes.[47,50] The observed higher number of branches in AD patients can possibly be due to the known abnormal vessel branching and angiogenesis induced by amyloid plaque deposition in vessel walls. The progressively heightened vascular complexity correlated with disease progression suggests that vascular geometry analysis of ToF MRA has potential to be used as an automated tool to study and characterize disease progression in AD and possibly other neurodegenerative diseases.

Limitations

Due to the inherent variability in the population, subject-specific vascular network alignments can deviate from the atlas in terms of the location of bifurcations and branches and averaging these anatomically variable networks in a Cartesian space can lead to errors. A larger dataset might mitigate this by including a larger number of outliers.

The extracted geometric properties are inherently affected by the source imaging resolution and region of interest (ROI) of the volume being imaged. The algorithm identifies vessels with a diameter as small as the imaging resolution; therefore, a higher resolution and larger imaging ROI increase the number of vessels detected, affecting the geometric properties such as total length and number of branches. The difference in spatial resolution of the MIDAS ($0.5\times0.5\times0.5$ mm^3) and OASIS-3 ($0.3\times0.3\times0.3$ mm^3) datasets may explain the lower average values for total length, volume, and the number of branches for healthy adults derived from MIDAS. To increase the number of scans comprising the atlas and in turn increasing the robustness of the atlas, we downsampled the 66 healthy MRA scans from the OASIS-3 database (from $0.3\times0.3\times0.3$ mm^3 to $0.5\times0.5\times0.5$ mm^3) to include in the averaged probabilistic atlas. However, to avoid any discrepancy in the data and maintain the cogency of our quantitative analysis', we restricted the comparison to data with the same imaging resolution. The features obtained from the stroke dataset (imaged at $0.5\times0.5\times0.5$ mm^3) were only compared to those of healthy subjects from the MIDAS data (imaged at $0.5\times0.5\times0.5$ mm^3), and the features of AD subjects were compared only to the healthy subjects within the OASIS-3 dataset (both imaged at $0.3\times0.3\times0.3$ mm^3).

Another inherent limitation of using multi-center clinical imaging data is that the volume or region of interest being scanned can vary between different studies and centers. The OASIS-3 dataset consisted of a larger scan volume and included a significant portion of the neck, leading to additional vasculature being detected. By limiting the ROI within the scanned volume of the OASIS-3 database we omitted the vascular segments corresponding to the neck region. This was done for consistency while creating the averaged probabilistic atlas and to only compare the vascular features specifically pertaining to the brain region.

Furthermore, we used MRA data of 45 patients with MCA and ICA occlusions to analyze cerebrovascular morphological changes in stroke patients. Although this sample represents the most common large vessel occlusion sites in AIS,[51] a larger sample size, including other proximal large and distal medium vessel occlusion sites, can improve our understanding of vascular architecture changes in stroke.

Conclusion

In conclusion, we developed a comprehensive atlas of healthy cerebrovascular morphology. Compared to healthy individuals, stroke and AD patients showed a significantly altered vascular morphology. The probabilistic atlas and extracted vascular morphometric features have the potential to be used as a non-invasive automated tool to study healthy aging and various pathological states, including prediction, diagnosis, surveillance, and treating cerebrovascular and neurodegenerative diseases. Further studies, including a larger sample size of various neurologic diseases and corresponding clinical data, are warranted to establish future clinical applications of the algorithm and atlas.

Acknowledgements and Disclosure:

This study was partially supported by the National Institutes of Health (NIH) National Institute of Neurological Disorders and Stroke (NINDS) award R03NS108167 and National Institute of Biomedical Imaging and Bioengineering (NIBIB) Trailblazer award R21EB032187. The findings of this manuscript are those of the authors and do not necessarily represent the official views of NINDS. The authors declare no competing interests.

Funding:

NIH NINDS grant number R03NS108167

References

1. World Health Organization. World Health Statistics. 2019.
2. Kalaria RN. Cerebral vessels in ageing and Alzheimer’s disease. Pharmacol Ther 1996;72:193–214. [PubMed: 9364575]
3. Wei F, Diedrich KT, Fullerton HJ, et al. Arterial tortuosity: An imaging biomarker of childhood stroke pathogenesis? Stroke 2016;47:1265–70. [PubMed: 27006453]
4. Arvanitakis Z, Capuano AW, Leurgans SE, Bennett DA, Schneider JA. Relation of cerebral vessel disease to Alzheimer’s disease dementia and cognitive function in elderly people: a cross-sectional study. Lancet Neurol 2016;15:934–43. [PubMed: 27312738]
5. Meyer EP, Ulmann-Schuler A, Staufenbiel M, Krucker T. Altered morphology and 3D architecture of brain vasculature in a mouse model for Alzheimer’s disease. Proc Natl Acad Sci U S A 2008;105:3587–92. [PubMed: 18305170]
6. Amukotuwa SA, Straka M, Smith H, et al. Automated detection of intracranial large vessel occlusions on computed tomography angiography a single center experience. Stroke 2019;50:2790–8. [PubMed: 31495328]
7. Sweeney MD, Montagne A, Sagare AP, et al. Vascular dysfunction—The disregarded partner of Alzheimer’s disease. Alzheimers Dement 2019;15:158–67. [PubMed: 30642436]
8. Wright SN, Kochunov P, Mut F, et al. Digital reconstruction and morphometric analysis of human brain arterial vasculature from magnetic resonance angiography. Neuroimage 2013;82:170–81. [PubMed: 23727319]
9. Liu J, Wang Y, Akamatsu Y, et al. Vascular remodeling after ischemic stroke: Mechanisms and therapeutic potentials. Prog Neurobiol 2014;115:138–56. [PubMed: 24291532]

10. Tanaka M, Sakaguchi M, Miwa K, et al. Basilar artery diameter is an independent predictor of incident cardiovascular events. Arterioscler Thromb Vasc Biol 2013;33:2240–4. [PubMed: 23661676]
11. Mukherjee D, Jani ND, Narvid J, Shadden SC. The role of Circle of Willis anatomy variations in cardio-embolic stroke: A patient-specific simulation based study. Ann Biomed Eng 2018;46:1128–45. [PubMed: 29691787]
12. Alastruey J, Parker KH, Peiro J, Byrd SM, Sherwin SJ. Modelling the circle of Willis to assess the effects of anatomical variations and occlusions on cerebral flows. J Biomech 2007;40:1794–805. [PubMed: 17045276]
13. Kalaria RN, Akinyemi R, Ihara M. Does vascular pathology contribute to Alzheimer changes? J Neurol Sci 2012;322:141–7. [PubMed: 22884479]
14. Toledo JB, Arnold SE, Raible K, et al. Contribution of cerebrovascular disease in autopsy confirmed neurodegenerative disease cases in the National Alzheimer's Coordinating Centre. Brain 2013;136:2697–706. [PubMed: 23842566]
15. Fischer VW, Siddiqi A, Yusufaly Y. Altered angioarchitecture in seleced areas of brains with Alzheimer's disease. Acta Neuropathol 1990;79:672–9. [PubMed: 2360411]
16. Barbará-Morales E, Pérez-González J, Rojas-Saavedra KC, Medina-Bañuelos V. Evaluation of brain tortuosity measurement for the automatic multimodal classification of subjects with Alzheimer's disease. Comput Intell Neurosci 2020;2020:4041832 [PubMed: 32405294]
17. Arvanitakis Z, Capuano AW, Leurgans SE, Bennett DA, Schneider JA. Relation of cerebral vessel disease to Alzheimer's disease dementia and cognitive function in elderly people: a cross-sectional study. Lancet Neurol 2016;15:934–43. [PubMed: 27312738]
18. Donato AJ, Machin DR, Lesniewski LA. Mechanisms of dysfunction in the aging vasculature and role in age-related disease. Circ Res 2018;123:825–48. [PubMed: 30355078]
19. Deshpande A, Jamilpour N, Jiang B, et al. Automatic segmentation, feature extraction and comparison of healthy and stroke cerebral vasculature. Neuroimage Clin 2021;30:102573. [PubMed: 33578323]
20. Chen L, Mossa-Basha M, Balu N, et al. Development of a quantitative intracranial vascular features extraction tool on 3D MRA using semiautomated open-curve active contour vessel tracing. Magn Reson Med 2018;79:3229–38. [PubMed: 29044753]
21. Kim BJ, Kim SM, Kang DW, Kwon SU, Suh DC, Kim JS. Vascular tortuosity may be related to intracranial artery atherosclerosis. Int J Stroke 2015;10:1081–6. [PubMed: 26061533]
22. Cool D, Chillet D, Kim J, Guyon JP, Foskey M, Aylward S. Tissue-based affine registration of brain images to form a vascular density atlas. Lect Notes Comput Sci 2003;2879:9–15.
23. Mouches P, Forkert ND. A statistical atlas of cerebral arteries generated using multi-center MRA datasets from healthy subjects. Sci Data 2019;6:29. [PubMed: 30975990]
24. Kerr D, Stanley JC, Barron M, Thomas R, Leatherdale BA, Pickard J. Symmetry of cerebral blood flow and cognitive responses to hypoglycaemia in humans. Diabetologia 1993;36:73–8. [PubMed: 8436257]
25. Zurada A, Gielecki JS. A novel formula for the classification of blood vessels according to symmetry, asymmetry and hypoplasia. Folia Morphol (Warsz) 2007;66:339–45. [PubMed: 18058758]
26. Zanto TP, Hennigan K, Östberg M, Clapp WC, Gazzaley A. Vessel tortuosity and brain tumor malignancy: A blinded study. Acad Radiol 2011;46:564–74.
27. LaMontagne P Longitudinal neuroimaging, clinical, and cognitive dataset for normal aging and Alzheimer disease. medRXiv 2019 [Epub ahead of print]
28. Morris JC, Weintraub S, Chui HC, et al. The Uniform Data Set (UDS): Clinical and cognitive variables and descriptive data from Alzheimer disease centers. Alzheimer Dis Assoc Disord 2006;20:210–6. [PubMed: 17132964]
29. Grabner G, Janke AL, Budge MM, Smith D, Pruessner J, Collins DL. Symmetric atlasing and model based segmentation: An application to the hippocampus in older adults. Med Image Comput Comput Assist Interv 2006;9:58–66
30. Brysbaert M, Stevens M. Power analysis and effect size in mixed effects models: A tutorial. J Cogn 2018;1:1–20

31. Blood Vessels of the Brain | Internet Stroke Center. http://www.strokecenter.org/professionals/brain-anatomy/blood-vessels-of-the-brain/. Accessed March 6, 2020.
32. Chandra A, Li W, Stone C, Geng X, Ding Y. The cerebral circulation and cerebrovascular disease I: Anatomy. Brain Circ 2017;3:35–40. [PubMed: 30276302]
33. Thissen D, Steinberg L, Kuang D. Quick and easy implementation of the Benjamini-Hochberg procedure for controlling the false positive rate in multiple comparisons. J Educ Behav Stat 2002;27:77–83.
34. van Vuuren AJ, Saling M, Rogerson S, Anderson P, Cheong J, Solms M. Cerebral arterial asymmetries in the neonate: Insight into the pathogenesis of stroke. Symmetry (Basel) 2022;14:456.
35. Bullitt E, Zeng D, Mortamet B, et al. The effects of healthy aging on intracerebral blood vessels visualized by magnetic resonance angiography. Neurobiol Aging 2010;31:290–300 [PubMed: 18471935]
36. Albers GW, Lansberg MG, Kemp S, et al. A multicenter randomized controlled trial of endovascular therapy following imaging evaluation for ischemic stroke (DEFUSE 3). Int J Stroke 2017;176:139–48.
37. Stryker Neurovascular. Clinical mismatch in the triage of wake up and late presenting strokes undergoing neurointervention with Trevo (DAWN). Stroke 2018;49:498–500. [PubMed: 29242390]
38. Ren Y, Chen Q, Li ZY. A 3D numerical study of the collateral capacity of the Circle of Willis with anatomical variation in the posterior circulation. Biomed Eng Online 2015;14:S11. [PubMed: 25603312]
39. Arjal RK, Zhu T, Zhou Y. The study of fetal-type posterior cerebral circulation on multislice CT angiography and its influence on cerebral ischemic strokes. Clin Imaging 2014;38:221–5. [PubMed: 24602416]
40. van Seeters T, Hendrikse J, Biessels GJ, et al. Completeness of the circle of Willis and risk of ischemic stroke in patients without cerebrovascular disease. Neuroradiology 2015;57:1247–51 [PubMed: 26358136]
41. Aiyagari V, Philip GB. Hypertension and stroke: pathophysiology and management. In: White WB, ed. Clinical Hypertension and Vascular Disease. Humana Press; 2016.
42. Sarmento RM, Vasconcelos FFX, Filho PPR, Wu W, De Albuquerque VHC. Automatic neuroimage processing and analysis in stroke - a systematic review. IEEE Rev Biomed Eng 2020;13:130–55. [PubMed: 31449031]
43. Alaka SA, Menon BK, Brobbey A, et al. Functional outcome prediction in ischemic stroke: A comparison of machine learning algorithms and regression models. Front Neurol 2020;11:889. [PubMed: 32982920]
44. Saver JL, Chapot R, Agid R, et al. Thrombectomy for distal, medium vessel occlusions: A consensus statement on present knowledge and promising directions. Stroke 2020;51:2872–84. [PubMed: 32757757]
45. Hughes TM, Craft S, Lopez OL. Review of “the potential role of arterial stiffness in the pathogenesis of Alzheimer’s disease”. Neurodegener Dis Manag 2015;5:121–35. [PubMed: 25894876]
46. Santos CY, Snyder PJ, Wu WC, Zhang M, Echeverria A, Alber J. Pathophysiologic relationship between Alzheimer’s disease, cerebrovascular disease, and cardiovascular risk: A review and synthesis. Alzheimers Dement (Amst) 2017;7:69–87 [PubMed: 28275702]
47. Govindpani K, McNamara LG, Smith NR, et al. Vascular dysfunction in Alzheimer’s disease: A prelude to the pathological process or a consequence of it? J Clin Med 2019;8:651.
48. Diagnosis and Treatment of Clinical Alzheimer’s-Type Dementia. Eff Heal Care Progr 2020;223:20-EHC003
49. Klohs J, Rudin M, Shimshek DR, Beckmann N. Imaging of cerebrovascular pathology in animal models of Alzheimer’s disease. Front Aging Neurosci 2014;6;32. [PubMed: 24659966]
50. El Tannir El Tayara N, Delatour B, Volk A, Dhenain M. Detection of vascular alterations by in vivo magnetic resonance angiography and histology in APP/PS1 mouse model of Alzheimer’s disease. MAGMA 2010;23:53–64. [PubMed: 20066469]

51. Saver JL, Goyal M, Van Der Lugt A, et al. Time to treatment with endovascular thrombectomy and outcomes from ischemic stroke: Ameta-analysis. JAMA 2016;316:1279–88 [PubMed: 27673305]

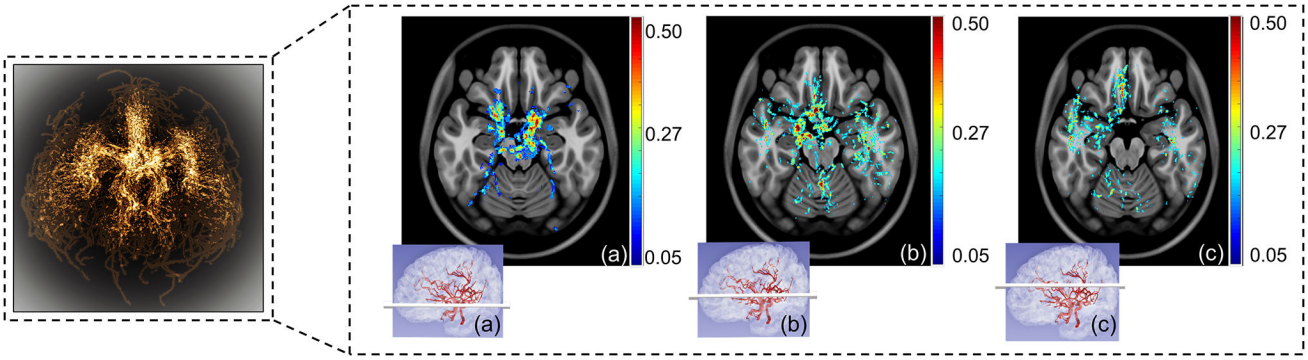

Figure 1.

The probabilistic atlas – selected axial slices showing the varying probability of arterial occurrence. The left panel shows the maximum intensity projection of the 3D probabilistic atlas with brighter regions corresponding to higher probability values based on vessel occurrence in the healthy cohort studied. The purple inserts (a), (b) and (c) represent the corresponding anatomical position of the axial slice shown.

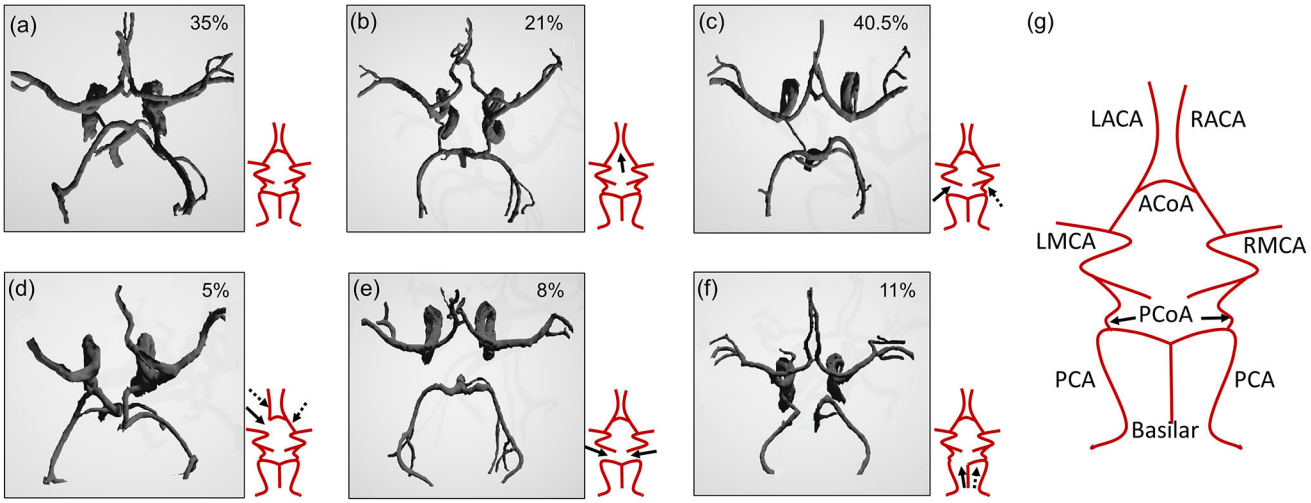

Figure 2.

The 6 most commonly occurring variations in the CoW anatomy of our healthy dataset. (a) Fully connected and formed CoW, (b) ACoA missing, (c) one of the PCoA missing, (d) A1 segment of ACA missing, (e) both of the PCoA missing, (f) P1 segment of PCA from Basilar missing. The arrows depict the missing segments (dashed arrows imply the possibility of the other equivalent segment being missing as well as the one shown by the solid arrow) and (g) a labeled schematic representation of the fully formed CoW, showing all the major vessel segments. The percentage values in the top right corner of each panel corresponds to the frequency of occurrence of that model within the healthy population used to study the variations.

ACoA: Anterior communicating artery; PCoA: Posterior communicating artery; L: Left; R: Right; ACA: Anterior cerebral artery; MCA: Middle cerebral artery.

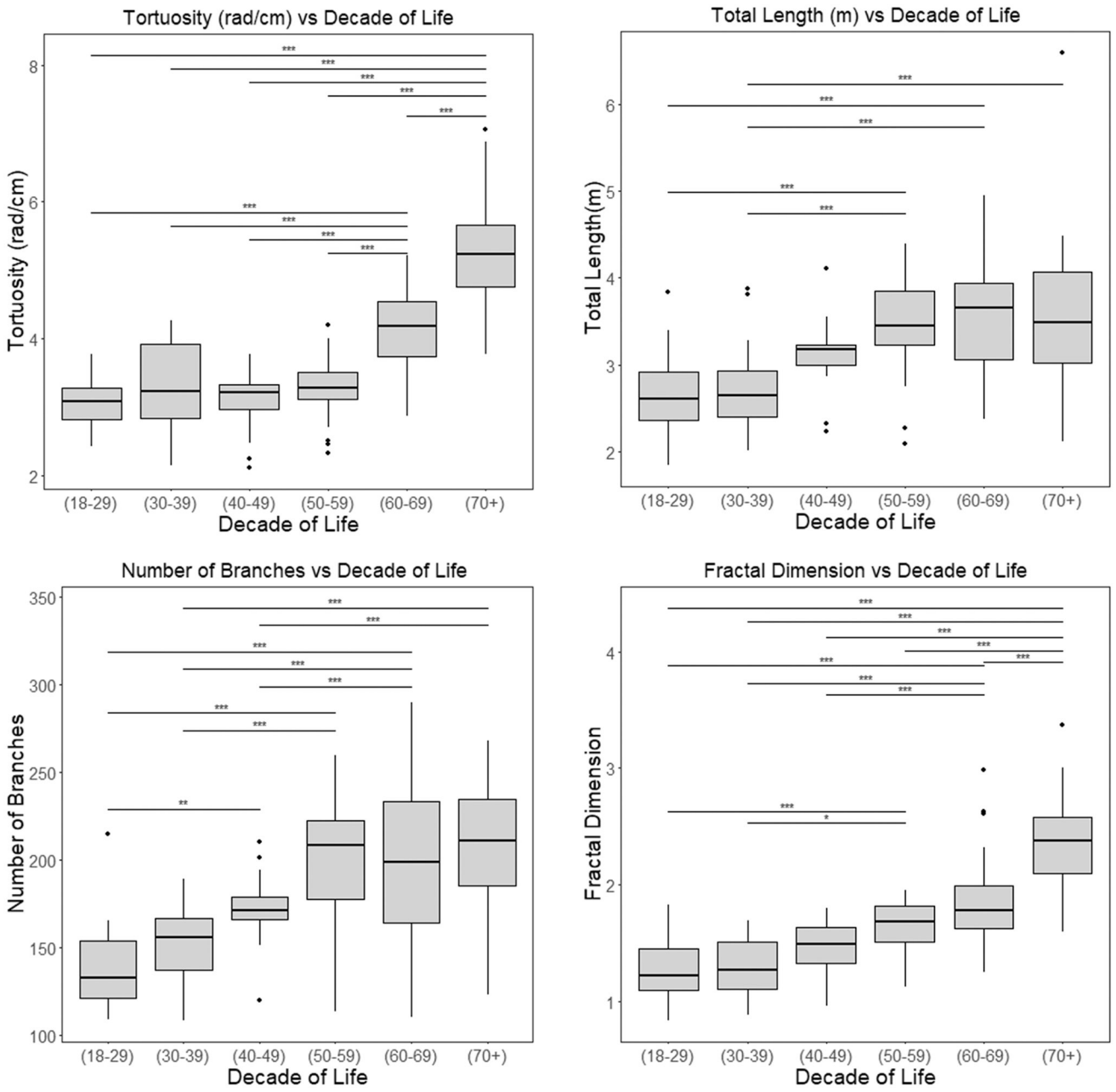

Figure 3.

Major findings of the effect of aging conducted on the healthy subjects from the atlas, demonstrating a significant change in vascular patterns with increasing age (in years) in certain vascular features. The ANOVA test results between age groups for the significantly different groups are represented by * for $p<0.05$, ** for $p<0.01$ and *** for $p<0.001$. The multi-group ANOVA had $p<0.001$ for tortuosity, number of branches and fractal dimension. rad: radians

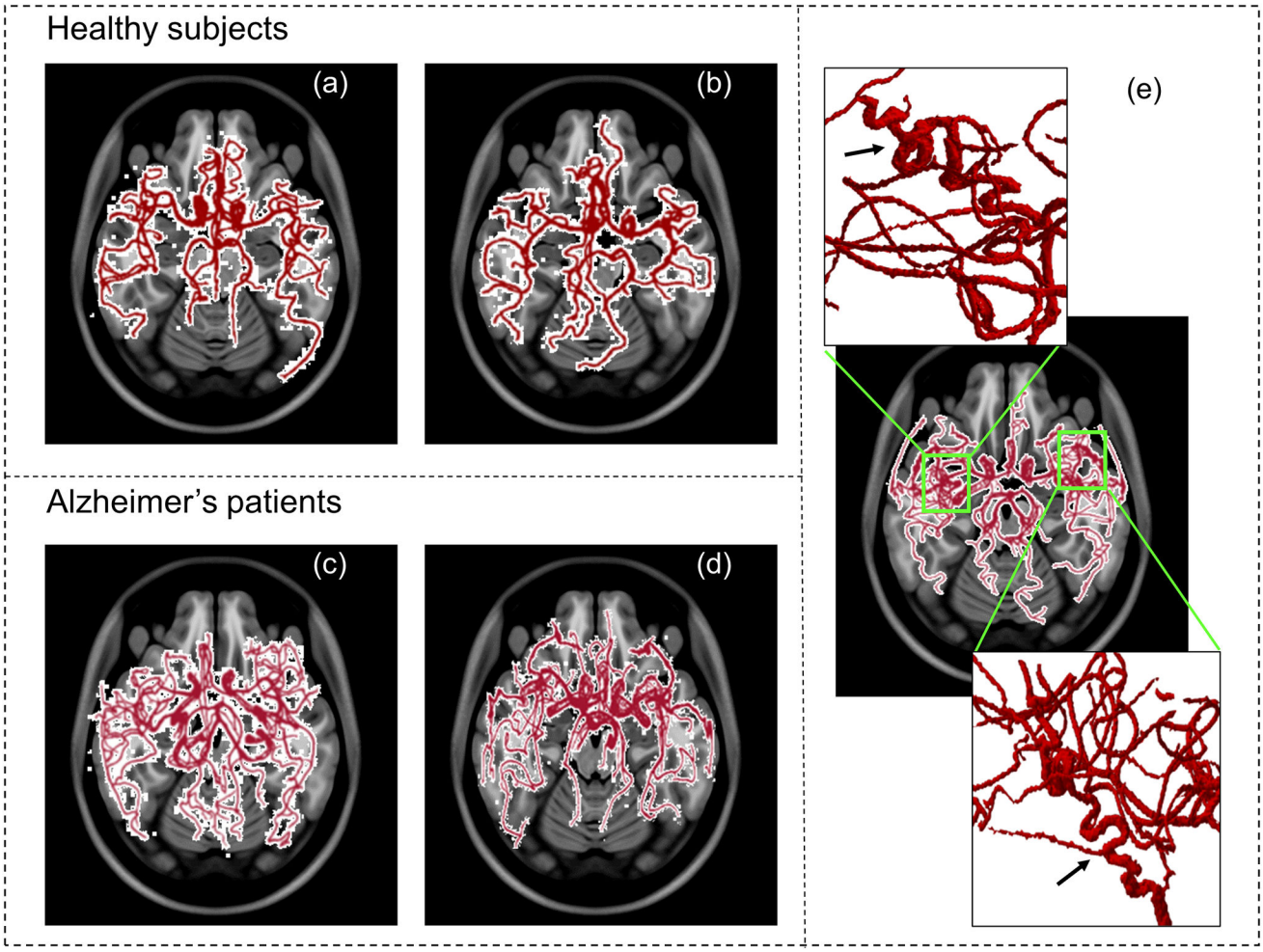

Figure 4.

Cerebral vascular network from 2 healthy subjects (a) and (b) and 2 AD patients (c) and (d) for visual comparison. We can see increased branching and vessel complexity in the AD patients, as compared to the healthy subjects. In panel (e), we can see the elevated tortuosity including looping and twisting in the highlighted region of the vascular network of an AD patient.

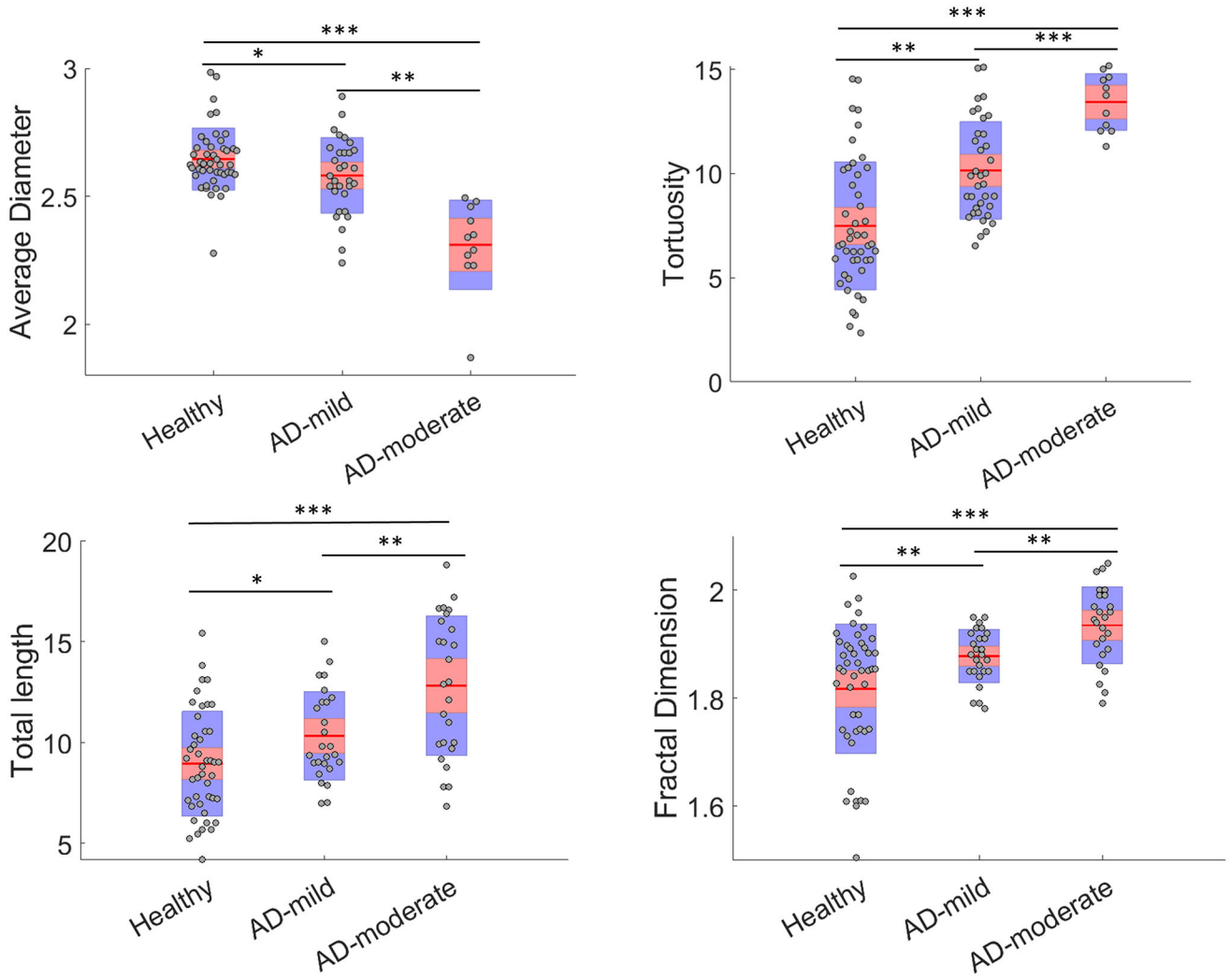

Figure 5.

The scatter plots of vascular geometrical features of the healthy subjects, early-mild, and moderate-severe Alzheimer's disease (AD). The red horizontal lines and shaded regions represent the mean and one standard deviation, respectively. The ANOVA test results between age groups for the significantly different groups are represented by * for $p<0.05$, ** for $p<0.01$ and *** for $p<0.001$.

Table 1.

The imaging material for the study.

	N (Female)	Age in years (Mean ± Standard Deviation)	Modality	Resolution
Healthy Subjects	109 (57) 66 (29)	30 ± 9.3 77 ± 9.7	ToF, T1	$0.5 \times 0.5 \times 0.5$ mm^3 $0.3 \times 0.3 \times 0.3$ mm^3
Ischemic Stroke	45 (20)	53 ± 16.1	ToF	$0.5 \times 0.5 \times 0.5$ mm^3
Alzheimer's Disease	50 (28)	75 ± 7.3	ToF	$0.3 \times 0.3 \times 0.3$ mm^3

N= Number of subjects; ToF: Time-of-Flight

Table 2.

The average features of the vascular tree of 175 healthy adults and the average percentage difference between the left and right hemispheric vascular geometric features within the healthy subject databases

	Average global features	Left vs. right hemisphere average difference %
Total length (m)	3.30 ± 0.65	30.57 ± 13
Number of branches	178.6 ± 30.62	18.06 ± 4.09
Average branch length (mm)	18.79 ± 5.67	31.15 ± 6.75
Maximum branch length (mm)	121.50 ± 21.02	23.36 ± 4.56
Average diameter (mm)	2.36 ± 0.34	3.21 ± 0.56
Total volume (ml)	89.92 ± 17.78	26.04 ± 9.44
Fractal dimension	1.64 ± 0.37	11.09 ± 0.97
Tortuosity (rad/cm)	4.17 ± 1.03	16.16 ± 2.76

All the data represent mean±standard deviation unless otherwise indicated. rad: radians

Table 3.

A comparison of geometric features of the cerebral vascular tree of healthy subjects and Stroke patients

	Healthy subjects	Stroke patients	p - value
Total length (m)	3.30 ± 0.65	2.10 ± 0.71	0.021 *
Number of branches	178.6 ± 30.62	166 ± 75.69	0.019 *
Average branch length (mm)	18.79 ± 5.67	12.58 ± 2.07	0.059
Maximum branch length (mm)	121.50 ± 21.02	59.38 ± 6.10	0.07
Average diameter (mm)	2.36 ± 0.34	2.18 ± 0.38	0.039 *
Total volume (ml)	89.92 ± 17.78	63.45 ± 21.83	0.009 *
Fractal dimension	1.64 ± 0.37	1.79 ± 0.20	0.027 *
Tortuosity (rad/cm)	4.17 ± 1.03	5.80 ± 0.92	0.041 *

All the data represent mean±standard deviation unless otherwise indicated. The significantly different features ($p<0.05$) are highlighted with a *. The p-values were corrected by the Benjamini-Hochberg method to control for the false detection rate. rad: radians

Table 4.

A comparison of geometric features of the cerebral vascular tree of healthy subjects and AD patients.

	Healthy subjects	AD patients (CDR = 0.5, 1)	AD patients (CDR = 2)	p - value
Total length (m)	3.92 ± 0.90	4.41 ± 1.41	5.21 ± 1.86	0.011 *
Number of branches	238 ± 118	283 ± 126	369 ± 145	0.079
Average diameter (mm)	2.23 ± 0.34	1.98 ± 0.31	1.74 ± 0.29	0.022 *
Fractal dimension	1.78 ± 0.24	1.86 ± 0.19	1.91 ± 0.25	0.016 *
Tortuosity (rad/cm)	6.74 ± 2.96	8.03 ± 3.11	10.27 ± 3.48	0.027 *

All the data represent mean±standard deviation with varying clinical dementia rating (CDR) unless otherwise indicated. The p-values were corrected by the Benjamini-Hochberg method to control for the false detection rate. The significantly different features ($p<0.05$) are highlighted with a *. rad: radians